Photocatalytic Degradation of Endocrine Disruptor Compounds in Water over Immobilized TiO$_2$ Photocatalysts

Zatloukalová, K.; Obalová, L.; Kočí, K.*+

Institute of Environmental Technology and Faculty of Metallurgy and Material Engineering,
VŠB - Technical University of Ostrava, 17. listopadu 15/2172, 708 33 Ostrava – Poruba, Czech Republic

Čapek, L.

Department of Physical Chemistry, Faculty of Chemical Technology, University of Pardubice, Studentská 95,
532 10 Pardubice, Czech Republic

Matěj, Z.

Department of Condensed Matter Physics, Faculty of Mathematics and Physics, Charles University in Prague,
Ke Karlovu 5, Prague 2 121 16, Czech Republic

Šnajdhaufová, H.

Institute of Chemical Process Fundamentals CAS, Rozvojová 135, Prague, Czech Republic

Ryczkowski, J.; Słowik, G.

Faculty of Chemistry, Maria Curie-Skłodowska University (UMCS), Pl. M. Curie-Skłodowskiej 5,
20-031 Lublin, POLAND

ABSTRACT: *Recently, the fate of endocrine disruptors in environmentally relevant samples has attracted considerable attention. Semiconductor photocatalysis may offer an appealing methodology to treat such contaminants. In this respect, the simultaneous degradation of synthetic hormones employing UV irradiation and TiO$_2$ as the photocatalyst were investigated. Our interest was focused on designing a photocatalytic reactor and finding a way to immobilize a powder photocatalyst by water-glass. The nanofiber powder photocatalyst NnF Ceram TiO$_2$ was chosen as powder photocatalysts based on TiO$_2$. The material was characterized by N$_2$ adsorption/desorption, XRD, UV-Vis spectrometry, and TEM. The reaction kinetics of hormone decomposition corresponds to a first-order reaction rate. It was shown that progesterone and all types of estradiols were decomposed most effortlessly in the presence of NnF Ceram TiO$_2$ photocatalysts. On the other hand, the lowest conversion was reached for estrone and estriol. The photocatalysts based on TiO$_2$ immobilized by water-glass seems to be promising for photocatalytic water purification.*

KEYWORDS: *Endocrine disruptors, Water purification, Photocatalysis, NnF Ceram TiO$_2$, Electric energy per order.*

INTRODUCTION

Water, together with the atmosphere, is a sine qua non for the existence of life on Earth. It is a chemical compound with two hydrogen atoms and one oxygen atom. Commonly, other substances are also dissolved in it, especially salts. In total, 97% of Earth's water is salty. Fresh water represents only 3% of Earth's water, most of which is in glaciers. Other than salts, other substances are found in water that may degrade its quality. Civilization and its activities seriously damaged 41% of the world's seas. The worst affected areas are the North and Mediterranean Seas, as well as the sea surrounding China, the Caribbean Sea and the east coast of North America. Only 4% of the world's oceans are relatively untouched, and these waters can be found near the world's poles. In the 20th century, 50% of the world´s wetlands disappeared [1].

Currently, approximately 1.2 billion people live in areas with natural water shortages. Another 1.6 billion people suffer from water shortages due to insufficient infrastructure. One-fifth of humans have no access to safe water. Drinking water consumption per person in Western Europe is approximately 129 litres. One US inhabitant consumes 295 litres of drinking water per day, whereas one person needs only approximately 20 litres in the dry regions of Africa. A five-minute shower uses the same amount of water as one person in a day in the slums in developing countries. The manufacture of one automobile uses approximately 2000 litres of water, the production of one kilogram of steel requires 18 litres of water, and one sheet of paper requires approximately 3 litres of water [2].

Three million people die each year from diseases caused by contaminated water and poor hygiene, 90% of them are children under five years of age. It is an unpleasant fact that the sources of fresh water on Earth continue to decrease. According to the estimates of the Food and Agriculture Organization, the water supply in Europe decreased by one-third, in Asia by three-quarters, and in Africa by two-thirds. Differences between water reserves and their consumption are continuously deepened, and it can be assumed that water consumption in the coming years will continue to rise. It is clear that, without water, civilization would not have reached such an advanced state of development—but does this really represent forward progress?

People should live every day with the basic points of the European Water Charter, which was adopted on May 6, 1968, in Strasbourg by the Council of Europe. This document summarizes the importance of water for humans and the environment and highlights the seriousness of the issue of water management [3].

The value of water is not only economic but is also ecological, and water is increasingly becoming a strategic raw material. Water demand is increasing with population growth, industrialization and the expansion of irrigation in agriculture. Therefore, wastewater purification has become essential for the preservation and expansion of water supplies. Conventional municipal wastewater treatment plants, usually based on biological processes, are able to remove some common pollutants, whereas biologically non-degradable compounds can escape and be released into the environment [4]. Among these compounds are endocrine disruptors. Disruption of the endocrine system in living organisms by synthetic organic chemicals has become a great concern in recent years due to the recognition that the environment is contaminated with numerous ''Endocrine Disrupting Compounds'' (EDCs) that exert hormonal activity [5]. Endocrine disruptors are found in many products with which we come into contact every day, such as cash receipts in supermarkets, beverage cans, floor coverings or sunscreens. Groups of endocrine disruptors include some heavy metals, phthalates, parabens, DDT, bisphenol A, PolyChlorinated Biphenyls (PCBs), pesticides, drugs or hormones. Hormones, even in very low concentrations, have the ability to interact with the endocrine systems of organisms, thus leading to a variety of developmental and reproductive disorders, as well as feminizing effects. Therefore, to eliminate these substances and ensure the quality of water, effective advanced purification methods are required [6]. Photocatalytic applications have gained particular attention for the degradation of hazardous contaminants and microorganisms. The photocatalyst TiO_2 has received increasing attention related to the degradation of organic pollutants due to its low cost, chemically stability, highly active photocatalytic properties, antibacterial ability and low toxicity to humans and the environment. It is expected that TiO_2 photocatalysis by themselves can be practically used in environmental decomposition technologies of endocrine disruptors and other dangerous substances [7-11].

Thus, photocatalytic degradation of certain hormones in the presence of immobilized TiO_2 photocatalysts was solved in this study. Some reasonable applications of the developed technology were looked for like a pilot project. The developed technology for decomposing undesirable substances could be practically used for cleaning water in whirlpools.

EXPERIMENTAL SECTION

Materials and reagents

The NnF Ceram TiO_2 photocatalyst was purchased from the company Pardam s.r.o. It is a white ceramic polycrystallic nanofiber powder. The hormones 17α-ethinylestradiol, 17α-estradiol, 17β-estradiol, estriol, estrone and progesterone were analysed. They were obtained from commonly available hormonal drugs:

- Cilest (0,035 mg of ethinylestradiolum in one tablet).
- Estrofem (1 mg of estradiolum in one tablet).
- Ovestin (1 mg of estriolum in one tablet).
- Agolutin (30 ml of progesterone in 1 mL).

The dosage for 80 litres of water was 20 tablets of Cilest and Estrofem, 30 tablets of Ovestin and 6 mL of Aglutin. No source of pure estrone was used. Estrone is an oxidation product of the 17 beta-estradiol.

Catalyst characterization

The TiO_2 photocatalyst was characterized by various techniques to specify their structural and textural properties: the crystalline phase and crystallite size by X-Ray Diffraction (XRD), specific surface area by nitrogen physical adsorption at 77 K, absorption properties by UV-vis absorbance and morphology by Transmission Electron Microscopy (TEM).

The surface area and porous structure of the photocatalysts were determined by adsorption/desorption of nitrogen at -196 °C using an ASAP 2010 instrument (Micromeritics, USA) and evaluated by the BET and BJH methods, respectively. Prior to the adsorption measurement, all of the samples were degassed at 110 °C until a pressure level of 0.1 Pa was attained (~ 24 h).

X-Ray Diffraction (XRD) analysis allows the determination of the crystalline sample composition and its microstructure (Masilko, 2015). XRD powder diffraction patterns were measured using a PANalytical MPD diffractometer in the conventional Bragg-Brentano setup, using Ni-filtered CuKa radiation, variable divergence and anti-scatter slits, 0.04 rad axial Soller slits and a PIXcel detector. NIST LaB_6 standard reference material (660a) was used for the instrumental broadening calibration. XRD data analysis, focused on the determination of lattice parameters/cell volume and crystallite size, was performed using the Rietveld/WPPM [12]] implemented in the software MSTRUCT MSTRUCT [13,14]. Models described in [15] were used.

The reflectance spectra measured by UV-Vis spectrophotometers can specify the width of the band gap semiconductor (Eg). UV–Vis diffuse reflectance spectra of catalysts were measured in quartz cuvettes (thickness 5 mm) by using a GBS CINTRA 303 spectrometer (GBC Scientific Equipment, Australia) equipped with an integrating sphere covered by a $BaSO_4$ layer. The spectra were recorded against spectralon reference material in the wavelength range of 200 to 900 nm (lamps switched at 350 nm). The scan rate was 100 nm/min. The scan step was 1 nm, and the width of the monochromator slit was 2 nm. The absorption was calculated from the reflectances using the Kubelka–Munk equation:

$$F(R_\infty) = (1 - R_\infty)^2/2.R_\infty, \tag{1}$$

where R_∞ is the diffuse reflectance from a semi-infinite layer.

Transmission Electron Microscopy (TEM) enables the observation of samples with a thickness of up to 100 nm at high magnification and high resolution. The catalyst sample was ground, and the resulting powder was poured with 99.8% ethanol to form a slurry. The sample was inserted into an ultrasonic homogenizer for 20 s. Then, the slurry containing the catalyst was pipetted and supported on a 200 mesh copper grid covered with lacey formvar and stabilized with carbon (Ted Pella Company) and left on the filter paper until the ethanol evaporated. Subsequently, the sample deposited on the grid was inserted on a holder and moved to the electron microscope. The electron microscope (Titan G2 60-300 kV FEI Company) was equipped with the following: Field Emission Gun (FEG), monochromator, three-condenser lens system, objective lens system, image correction (Cs-corrector), HAADF detector and an EDS spectrometer (Energy Dispersive X –Ray Spectroscopy; EDAX Company) with a Si(Li) detector used to display the prepared catalysts. Microscopic studies of the catalysts were carried out at an accelerating voltage of the electron beam equal to 300 kV.
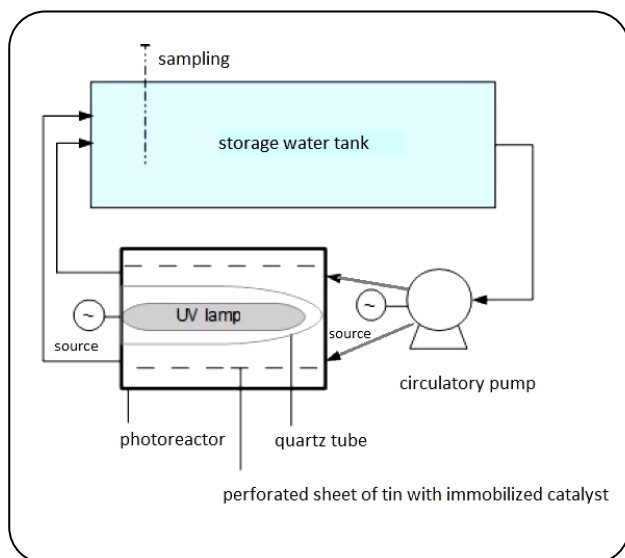
Fig. 1: Scheme of experimental apparatus.

Experimental apparatus

The photocatalytic degradation of endocrine disruptors was carried out in a homemade apparatus. The apparatus consisted of three main parts, namely, the batch photoreactor with circulation, the pump and the water tank. The scheme is shown in Fig. 1. The design and construction was arranged by the company TAW s.r.o.

A stirred (by pump) batch annular reactor (length 465 mm, width 160 mm) with an immobilized photocatalyst was illuminated by a 36 W UV lamp with a peak light intensity at 368 nm (Lynx-L 36W BL368 co. Havells Sylvania) situated in the centre of the photoreactor.

The intensity of the lamp was measured by radiometer MS-100 Multisense Optical Radiometer. The temperature during testing was 20 °C. Measuring was done on the top, in the middle and on the bottom part of the lamp. These three values were averaged. From getting data resulted that the intensity is sinking with rising distance from the light source. Maximum distance between the catalyst carrier and the quartz tube with lamp is 1 cm. Testing distance was 0.8 cm. Temperature was monitored at the beginning when the hormones were applied to the water and then before taking the samples for analysis.

The material used for the jacket reactor was aluminium, and the part was polished to ensure maximum reflectance of light [16]. For the design of the photoreactor dimensions, namely, the distance between the carrier with photocatalysts and the lamps, it was necessary to measure how the intensity of radiation of the selected lamp changes with distance and also to make sure that the intensity of the radiation is not too strong. A quartz tube with a diameter of 10 cm was utilized for the construction of the reactor, and the carrier of photocatalyst was at a distance of 0.8 cm from the quartz tube. The internal volume of the photoreactor was 5.23 dm^3. The water was pumped to the reactor from a reservoir with a volume of 181 litres by a circulation pump with a flow rate of 3.7 L/min.

A perforated plate with a mesh diameter of 1.5 mm and a distance between meshes of 2.5 mm was selected as a suitable carrier based on testing. A suitable method of immobilization of the TiO$_2$ catalyst seems to be water-glass immobilization because of its inorganic character and better mechanical resistance in comparison with other inorganic adhesives. Organic adhesives were excluded because of their degradation during photocatalysis. After coating the carrier with a water-glass layer, 1.5 g of catalyst was spread on it and then dried at 200 °C.

Analytical methods

For the identification of the degradation of hormones, the samples taken during the photocatalytic experiments were analysed by the Liquid Chromatography/ Mass Spectrometry/ Mass Spectrometry (LC/MS/MS) method. The sampling and subsequent analytical data were provided by the company Povodí Odry s.p. The temperature was monitored at the beginning when the hormones were applied to the water and then before taking the samples for analysis.

RESULTS AND DISCUSSION
Characterization of catalysts

The specific surface area S_{BET} of the tested sample was 30 m^2/g (Table 1).

The structural and microstructural properties of the explored photocatalyst evaluated from X-ray diffraction patterns (Fig. 2) are summarized in Table 1. From Fig. 2, it can be revealed that the NnF Ceram TiO$_2$ photocatalyst is not only the anatase crystalline phase but may also be a mixture of anatase, rutile and brookite. For XRD data fitting, the anatase crystallites were assumed to be spherical, with diameters distributed according to the log-normal distribution [12]. The refined crystallite-size is reported in Table 1.

Table 1: The basic textural, optical and structural characterizations of tested samples.

Sample	S_{BET} (m²/g)	XRD phase character	Phase composition	Crystallite size (nm)	Band gap energy (eV)
NnF Ceram TiO₂	30	crystalline	68 wt.% anatase + 7 wt.% rutile + 25 wt.% brookite	10.5*/ 23*/ 4,3*	3.15
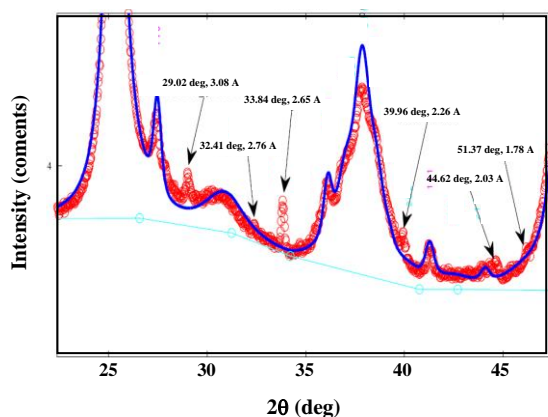
Fig. 2: XRD patterns of NnF Ceram TiO₂ catalyst.

The band gap value of photocatalyst (Table 1) was determined by UV-Vis spectroscopy. The value obtained for the band gap energy of the NnF Ceram catalyst was 3.15 eV. From these values, it is evident that the value of band gap energy for NnF Ceram is lower than pure anatase, so this photocatalyst needs radiation with lower energy (higher wavelength) for he excitation of electrons, which means that there is a shift of adsorbed radiation towards the visible region. Such a circumstance should subsequently have a positive effect on the photocatalytic properties of the NnF Ceram photocatalyst. A band gap energy of anatase between 3.20 and 3.56 eV was published in the literature, and the energy for rutile is between 3.00 and 3.34 eV [17], which corresponds to wavelengths of 388 nm and 413 nm, respectively. It follows that the value of the band gap for the catalyst NnF Ceram corresponds to the band gap energy of anatase. This can be explained by the fact that the band gap energy is not only determined by the presence of anatase or rutile but also by the properties of anatase alone (such as the particle size, for example). This also follows from a wide range of energy band gaps published for anatase (3.20 to 3.56 eV).

The nanofiber catalyst NnF Ceram was studied by transmission electron microscopy. The separation of crystallographic orientation in the TiO₂ sample was performed by Fast Fourier Transform (FFT) by using a masking available in the Gatan DigitalMicrograph software package. FFT was generated from the HRTEM images (Fig. 3 A). Based on FFT, the crystallographic orientations of planes in TiO₂ were defined. Application of a suitable mask on FFT allows the separation of one or more of the plane crystallographic directions from a HRTEM image. The eight most intense rings observed on FFT (Fig. 3 B) are assigned to the (101), (103), (004), (112), (200), (105), (211), and (204) reflections of the anatase phase [18-20]. The interplanar distances of 3.52 Å, 2.43 Å, 2.37 Å, 2.33 Å, 1.90 Å, 1.70 Å, 1.67 Å and 1.48 Å in the HRTEM image (Fig. 3 A) correspond to the (101), (103), (004), (112), (200), (105), (211) and (204) planes of the anatase crystal phase of TiO₂, respectively. The HRTEM image (Fig. 4) shows an interplanar distance of 3.52 Å, which matches well with the (101) planes of anatase TiO₂ [21]. A typical width of the nanorods, estimated based on TEM images (Fig. 5), ranged between 115.22 and 687.66 nm.

Photocatalytic activity

Testing the efficiency of the catalysts during the photocatalytic degradation of hormones was carried out without any prior treatment of water at a pH of approximately 7.8. The results of the analysis of water before the start of photocatalysis and after the 24-hour cycle with a total time of irradiation of 93 min and after the 48-hour cycle with a total time of irradiation of 186 min are shown in Tables 2. The measurement error was 17.6%.

Conversions of these hormones were calculated from measured data according to the equations

$$X_A = \frac{n_{Ao} - n_A}{n_{Ao}} \tag{2}$$

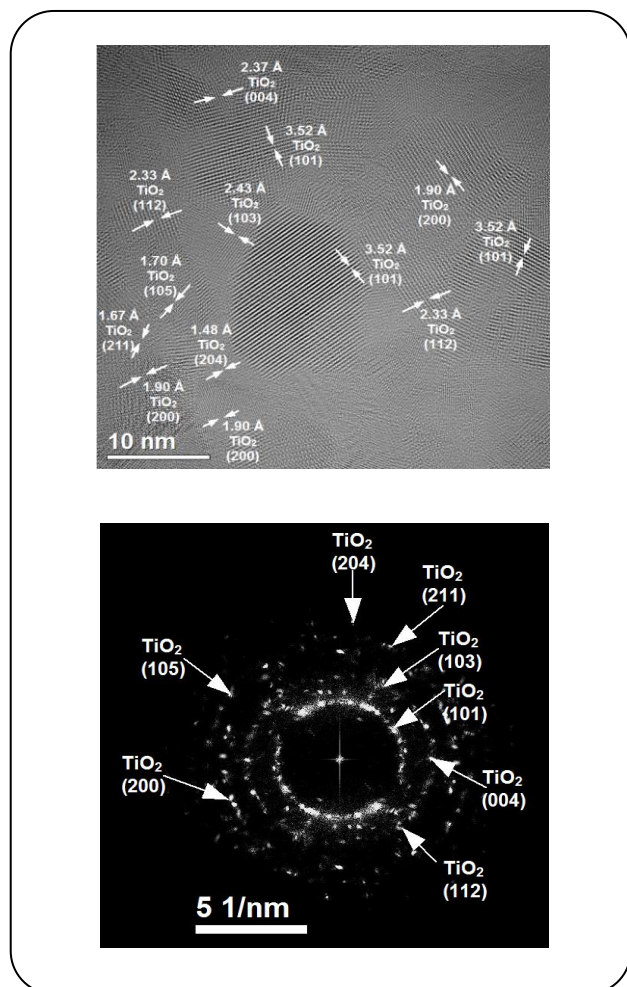$$X_A = \frac{C_{Ao} - C_A}{C_{Ao}} \qquad V = konst. \tag{3}$$

Fig. 3: (A) HRTEM image and (B) FFT with interplane distances NnF Ceram catalyst.
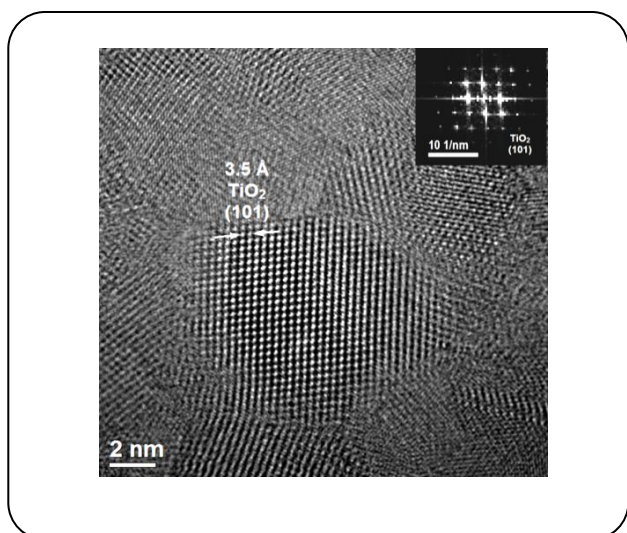

Fig. 4. Particular planes of NnF Ceram catalyst separated from HRTEM images (Fig. 3 A)

Where X_A is the degree of conversion, n_{A0} (mol) is the initial concentration of substance A, and n_A (mol) is the concentration of substance A at a set time. In the case of constant volume, we count c_{A0} (µg/L) as the initial concentration of substance A and c_A (µg/L) as the concentration of substance A at a set time. The calculated conversion values are plotted in the general diagram (Fig. 6), which clearly presents the conversion of all of the analysed hormones during the 24- and 48-hour cycles with total times of irradiation of 93 and 186 min, respectively.

Based on the results in Fig. 6, it is apparent that the NnF Ceram photocatalyst is effective in the degradation of hormones. The total degradation of progesterone was noticed after 48 hours. The conversion of estriol-based hormones was approximately 80%. The lower degrees of degradation of estriol and estrone occurred.

Favourable decompositions occurred in 17α-estradiol, 17β-estradiol (E2), 17α-ethinylestradiol (EE2), and progesterone. The lowest conversions were observed for estrone (E1) and estriol (E3). The tested oestrogens are eighteen carbon steroids with a phenolic group that is responsible for their estrogenic activity. While studying the degradation rates of E2, E1 and EE2, it was found that E2 was oxidized to E1 in the first step. Degradation of E1 must be initiated by the fission of a single carbon ring, which is a slow step. That is why the concentration of E1 at the outlet of the wastewater treatment plant is usually higher than the concentration of E2, although E2 is secreted in much larger quantities. E2 is removed relatively quickly, together with the formation of E1, which is then degraded more slowly. The degradation of E1 exhibits a linear relationship with the removal of estrogenic potential. The structure of EE2 is similar to E2, except that an ethynyl group is on one hydroxyl group that contains a carbon atom. We can therefore assume that the removal of EE2, as well as E2, will be under way [22].

Current studies of the photocatalytic degradation of oestrogens [23] report first-order kinetics. The reaction rate of each oestrogen in solution can be modelled by:

$$-r_i = k_{T,i} (LVRPA)^m c_i \qquad (4)$$

where $k_{T,i}$ is an apparent reaction rate constant that is independent of photon absorption in the reactor. The exponent m is equal to 0.5 in the presence of TiO₂,

Table 2: The results of analysis of water with content of hormones before and after the photocatalysis in the presence of a photocatalyst NnF Ceram.

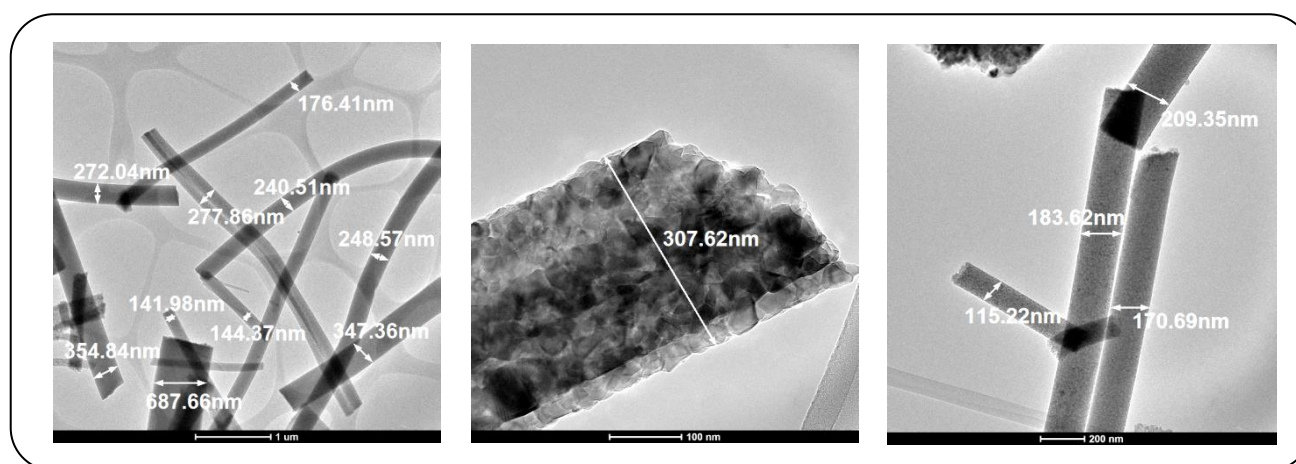| Hormones	Initial concentration (µg/L)	Concentration after 24 hours cycle with irradiation 93 min (µg/L)	Cncentration after 48 hours cycle with irradiation 186 min (µg/L)
17α -ethinylestradiol	2.9	2.4	2.2
17α-estradiol	6.7	4.9	3.8
17β-estradiol	44.0	34.0	25.0
estriol	190.0	180.0	170.0
estrone	66.0	65.0	61.0
progesterone	110.0	40.0	24.0

Fig. 5: TEM images of structures - width of nanofibers NnF Ceram catalyst.
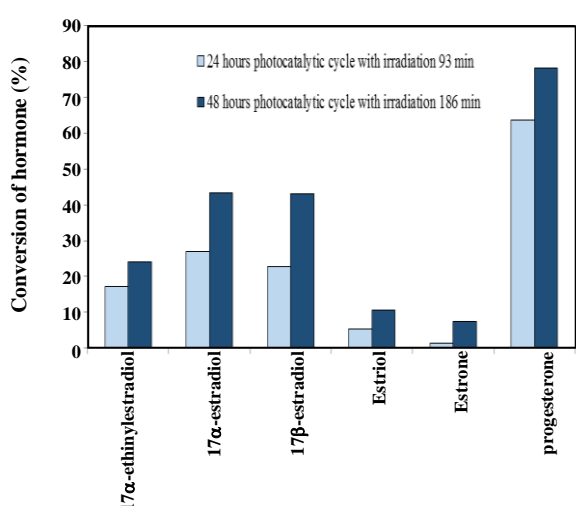

Fig. 6: Conversion of hormones during the photocatalytic affect of NnF Ceram photocatalyst.

LVRPA is the local volumetric rate of the absorption of photons (W/m^3), and c_i is the concentration of hormones (mol.m^3). Under such circumstances, there was no significant degradation of E3 or E1. However, 49%, 20% and 25% of E2 and EE2 were removed, respectively, after 180 minutes of irradiation. It is assumed that the rate of constant degradation of oestrogen is independent of the radiation absorbed in the photoreactor.

All of these assumptions are in accordance with results from the degradation of hormones from water with tested photocatalyst.

Electric Energy per Order (EEO)

Advanced oxidation technologies (AOTs), which involve the in situ generation of highly potent chemical

oxidants, such as the hydroxyl radical (•OH), have emerged as an important class of technologies for accelerating the oxidation (and hence removal) of a wide range of organic contaminants in polluted water and air. Standard figures-of-merit are proposed for the comparison and evaluation of these waste treatment technologies. The electric energy per order of magnitude (E_{EO}) is suitable to use for evaluating the efficiency of electrically controlled processes for low concentrations. This standard figure-of-merit provides a direct link to the electric-energy efficiency (lower values mean higher efficiency) of an advanced oxidation technology, independent of the nature of the system [24].

Although the removal and eventual mineralization of organic contaminants through advanced oxidation processes can be complex and involve a number of elementary chemical steps, the overall kinetics or rate of removal of a specific component can often be described phenomenologically by simple first-order kinetics:

$$\ln\left(c_0/c\right) = kt \tag{5}$$

where t is the reaction time in min, k is the first-order rate constant, c_0 is the initial concentration of the contaminant, and c is the concentration of the contaminant.

Electric energy per order (E_{EO}) is best used for situations where [C] is low (i.e., cases that are overall first-order in C) because the amount of electric energy required to bring about a reduction by one order of magnitude in [C] is independent of [C]. Thus, it would take the same amount of electric energy to reduce the contaminant concentration from 10 mg/L to 1 mg/L in a given volume, as it would to reduce it from 10 μg/L to 1 μg/L. Electric energy per order (E_{EO}) is the electric energy in kilowatt hours [kWh] required to degrade a contaminant by one order of magnitude in a unit volume (e.g., in 1 m^3 (1000 L)) of contaminated water or air.

E_{EO} values [usual units, kWh/m^3/order] can be calculated using the following formulas for batch operation:

$$E_{EO} = \frac{pt\,1000}{v\,iog\left(c_0/c\right)} \tag{6}$$

where P is the electric power [kW] of the irradiation source, t is the irradiation time [h], V is the volume [L] of treated water, c_0 is the initial concentration of contaminant, and c is the final concentration of contaminant.

When assuming the first order equation, the following can be applied:

$$\log\left(c_0/c\right) = 0.4343k_1't \tag{7}$$

where t is the reaction time in min and   is the first-order rate constant in min^{-1}.

For ideal batch reactors, the equation can be transformed as:

$$E_{Eo} = \frac{38.4P}{Vk_1'} \tag{8}$$

where V is the batch reactor volume [L].

From the above phenomena, the degradation of the hormones can be described with first-order kinetics, and calculated kinetic constants and half-lives were from the results of the photocatalytic degradation of tested hormones. These kinetic parameters and the calculated energy required for the reduction of pollutant concentration by one order (E_{EO}) are shown in Tables 3 for tested photocatalyst.

Calculated E_{EO} values are rather high, especially for estriol and oestrogen in the presence of tested photocatalyst. The energy calculation enables one to estimate the costs of the photocatalytic system and provides information on the overall performance and capital investment necessary for a particular application.

Concerning the treatment costs of the model pollutants, a rough estimation can be made using the EU-28 average electricity price for industrial consumers: 0.119 € per kWh (2/2013) (Eurostat 2014). Assuming a one-hour treatment time for the pollutants in the wastewater matrix in the presence of tested photocatalyst, the estimated prices are 20, 10, 11, 53, 80 and 4 €/per order for 17α- ethinylestradiol, 17α-estradiol, 17β-estradiol, estriol, estrone and progesterone, respectively.

CONCLUSIONS

Overall, the removal of hormones from wastewater under UV irradiation and in the presence of TiO$_2$ photocatalysts immobilized by water glass was investigated. Hence, the main conclusions drawn from this study are summarized as follows:

● The proposed photocatalytic device with an immobilized TiO$_2$ photocatalyst can be used for removing hormones from wastewater.

Table 3: Summary of the calculated kinetic constants and E_{EO} in the presence of NnF Ceram TiO$_2$ catalyst.

Hormone	k'_1 (10^3 min^{-1})	E_{EO} (kWh/m^3)
17α- ethinylestradiol	1.6	165
17α-estradiol	3.1	85
17β-estradiol	3.0	88
estriol	0.6	440
estrone	0.4	660
progesterone	8.7	30

● Progesterone and all types of estradiols were decomposed with the least amount of effort. On the other hand, the lowest conversion was reached for estrone and estriol.

Hence, photocatalytic treatment using immobilized TiO$_2$ photocatalysts is promising, with low energy requirements and an efficient process for removing endocrine disrupting compounds from aqueous matrices. The key advantage of the proposed setup is that there is no need for a photocatalyst after treatment and separation by the photocatalytic process, thus decreasing the overall cost of a large-scale treatment plant.

Acknowledgements

REFERENCES

[1] Rapantová N., Grmela A., "Voda – Strategická Surovina Pro 21. Století" Sborník 10. Česko – Slovenského Mezinárodního Hydrogeologického Kongresu, VŠB-TUO, Ostrava (2009).

[2] Kravčík M., Pokorný J., Kohutiar J., Kováč M., Tóth E., "Voda Pre Ozdravenie Klímy-Nová Vodná Paradigm", Krupa Print, Žilina (2007).

[3] European Water Charter https://rm.coe.int/CoERMPublicCommonsSearchSer vices/DisplayDCTMContent?documentID=0900001 6804d6d09

[4] Zhang X.J., Chen C., Lin P.F., Hou A.X., Niu Z.B., Wang J., Emergency Drinking Water Treatment During Source Water Pollution Accidents in China: Origin Analysis, Framework and Technologies. *Environ. Sci. Technol*. **45**: 16 – 167 (2010).

[5] Metzler M., Pfeiffer E., "Chemistry of Natural and Antropogenic Endocrine Active Compounds: Metzler, M. (Ed.), Endocrine Disruptors Part I", Springer, Germany (2001).

[6] Tabata A., Kashiwada S., Ohnishi Y., Ishikawa H., Miyamoto N., Itoh M., Magara Y. Estrogenic Influences of 17-Estradiol, p-Nonylphenol and Bisphenol A on Japanese Medaka (Oryzias latipes) at Detected Environmental Concentrations, *Water Sci. Technol*. **43**: 109–116 (2001).

[7] Fujishima, A., Honda, K., Electrochemical Photolysis of Water at a Semiconductor Electrode, *Nature* **288**: 37–38 (1972).

[8] Watanabe, T., Super Hydrophilic Photocatalyst and Its Application, *Bul. Ceram. Soc. Jpn.,* **31**: 837–840 (1996).

[9] Kottegoda I.R.M., Colombge H.C.D.P., Karunadasa K.S.P., Samarawickrama D.S., Manorathne C.H., An Efficient Reactor for Purification of Domestic Water Using Solar Energy, *Int. J. Energy Eng.*, **3**: 93-98 (2013).

[10] Ollis D.F., Photocatalytic Purification and Treatment of Water and Air, *Comptes Rendus de l'Academie des Sci. - Series IIC – Chem.,* **3**, 405–411 (2000).

[11] Gültekin I., Ince N.H., Synthetic Endocrine Disruptors in the Environment and Water Remediation by Advanced Oxidation Processes, *J. Environ. Manag*., **85**: 816–832 (2007).

[12] Scardi P., Leoni M., Whole Powder Pattern Modelling Acta Crystallogr. *Sect. A: Found. Crystallogr*. **58**: 190-200 (2002).

[13] Matěj Z., Kužel R., MStruct – Program / Knihovna Pro Mikrostruktury Analýzu Pomocí Práškové Difrakce. Available Online At: http://www.xray.cz/mstruct/ (2009).

[14] Matěj Z., Kužel R., Nichtová L., XRD Total Pattern Fitting Applied to Study of Microstructure of TiO$_2$ Films, *Powder Diff*., **25**(2): 125–131 (2010).

[15] Matěj Z., Matějová L., Kužel R., XRD Analysis of Nanocrystalline Anatase Powders Prepared by Various Chemical Routes: Correlations Between Micro-Structure and Crystal Structure Parameters, *Powder Diffr*., **28**: 161-183 (2013).

[16] Krystyník P., "Photochemical and Photocatalytic Oxidation Processes in Liquid Phase": Thesis. VŠCHT, Prague (2015).

[17] Nakaruk A., Ragazzon D., Sorrell C.C., Anatase–Rutile Transformation Through High-Temperature Annealing of Titania Films Produced by Ultrasonic Spray Pyrolysis, *Thin Solid Films,* **518**: 3735–3742 (2010).

[18] Vijayalakshmi R., Rajendran K.V., Effect of K$^+$ Doping on the Phase Transformation of TiO$_2$ Nanoparticles. *Adv. in Technol. of Materials and Materials Proc*., **12**(1): 25-30 (2010).

[19] Sun Ch.H., Yang X.H., Chen J.S., Li Z., Lou X.W., Li Ch., Smith S.C., Lu (Max) G.Q., Yang H.G., Higher Charge/Discharge Rates of Lithium-Ions Across Engineered TiO$_2$ Surfaces Leads to Enhanced Battery Performance, *Chem. Commun*., **46**: 6129-6131 (2010).

[20] Cui J., Sun D., Zhou W., Liu H., Hu P., Ren N., Qin H., Huang Z., Lina J., Ma H., Electrocatalytic Oxidation of Nucleobases by TiO$_2$ Nanobelts, *Phys. Chem*. **13**: 9232–9237 (2011).

[21] Chu L., Li L., Su J., Tu F., Gao N.L.Y., 2013. A General Method for Preparing Anatase TiO$_2$ Treelike-Nanoarrays on Various Metal Wires for Fiber Dye-Sensitized Solar Cells, *Sci. Rep*., **4**: 4420 (2013).

[22] Moschet, CH., ibp.ethz.ch. Available online at: http://www.ibp.ethz.ch/research/aquaticchemistry/teaching/archive_past_lectures/term_paper_08_09/HS08_CHRISTOPH_MOSCHET_rev_termpaper.pdf (2009).

[23] Puma G.L., Puddu V., Tsang H.K., Gora A., Toepfer B., Photocatalytic Oxidation of Multicomponent Mixtures of Estrogens (Estrone (E1), 17-Estradiol (E2), 17-Ethynylestradiol (EE2) and Estriol (E3)) under UVA and UVC Radiation: Photon Absorption, Quantum Yields and Rate Constants Independent of Photon Absorption, *Appl. Cat. B: Environ*. **99**: 388-397 (2010).

[24] Bolton J.R., Bircher K.G., Tumas W., Tolman C.A., Figures-of-Merit for the Technical Development and Application of Advanced Oxidation Technologies for Both Electric-and Solar-Driven Systems, *Pure Apl. Chem.,* **73**: 627–637 (2001).